Stem Cell Reports
Report

ISSCR

OPEN ACCESS

MiR-31/SDHA Axis Regulates Reprogramming Efficiency through Mitochondrial Metabolism

Man Ryul Lee,[1,2,4,*] Charlie Mantel,[1,4] Sang A. Lee,[2] Sung-Hwan Moon,[3] and Hal E. Broxmeyer[1,*]
[1]Department of Microbiology and Immunology, Indiana University School of Medicine, 950 West Walnut Street, Indianapolis, IN 46202-5181, USA
[2]Soonchunhyang Institute of Medi-bio Science, Institute of Tissue Regeneration, Soon Chun Hyang University, Asan-si, 31151 Chungcheongnam-do, Republic of Korea
[3]School of Medicine, Kon Kuk University, 05029 Seoul, Republic of Korea
[4]Co-first author
*Correspondence: leeman@sch.ac.kr (M.R.L.), hbroxmey@iupui.edu (H.E.B.)
http://dx.doi.org/10.1016/j.stemcr.2016.05.012

SUMMARY

Metabolism is remodeled when somatic cells are reprogrammed into induced pluripotent stem cells (iPSCs), but the majority of iPSCs are not fully reprogrammed. In a shift essential for reprogramming, iPSCs use less mitochondrial respiration but increased anaerobic glycolysis for bioenergetics. We found that microRNA 31 (miR-31) suppressed succinate dehydrogenase complex subunit A (SDHA) expression, vital for mitochondrial electron transport chain (ETC) complex II. MiR-31 overexpression in partially reprogrammed iPSCs lowered SDHA expression levels and oxygen consumption rates to that of fully reprogrammed iPSCs, but did not increase the proportion of fully reprogrammed TRA1-60$^+$ cells in colonies unless miR-31 was co-transduced with Yamanaka factors, which resulted in a 2.7-fold increase in full reprogramming. Thus switching from mitochondrial respiration to glycolytic metabolism through regulation of the miR-31/SDHA axis is critical for lowering the reprogramming threshold. This is supportive of multi-stage reprogramming whereby metabolic remodeling is fundamental.

INTRODUCTION

The majority of induced pluripotent stem cells (iPSCs) are not fully reprogrammed (Chan et al., 2009; Lee et al., 2013; Mikkelsen et al., 2008). There is still minimal information on transition checkpoints necessary to induce full reprogramming. Pluripotent stem cells (PSCs) have functions and requirements different from somatic cells. In contrast to somatic cells, PSCs have a shorter G_1 phase of the cell cycle and unlimited cell growth capacity, as in cancer stem cells (CSCs). While PSCs have metabolic activities very different from those of somatic cells to meet a proper balance between ATP production as an energy source and biosynthetic demands (Varum et al., 2011; Zhang et al., 2012), metabolic differences between partial (par) and fully (full) reprogrammed iPSCs are yet to be determined.

Increased glycolytic flux is characteristic of CSCs and embryonic stem cells (ESCs). They require increased ATP and anabolic precursors for rapid proliferation compared with normal somatic cells (Zhang et al., 2012). Metabolism of ESCs differs from CSCs; they contain lower numbers of mitochondria and less mtDNA (Folmes et al., 2012), and have less active oxidative phosphorylation (Folmes et al., 2011). ESCs are particularly vulnerable to oxygen radicals, which cause genomic damage, apoptosis, and decreased differentiation capacity (Han et al., 2008; Zhang et al., 2012). This is important for lower mitochondrial respiration in PSCs, because reactive oxygen species (ROS) generation is a consequence of electron transport chain (ETC) activity. Shifting to anaerobic glycolysis is a form of ROS defense. Somatic cells must switch mitochondrial oxidative metabolism to anaerobic glycolytic pathways during iPSC reprogramming (Folmes et al., 2011; Liu et al., 2013; Xu et al., 2013). However, little is known regarding molecular mechanisms involved in metabolic reprogramming.

We reported that CD34$^+$ cells from thawed human cord blood (CB) cryopreserved for more than 20 years could be successfully reprogrammed using lentiviruses expressing Yamanaka factors (Broxmeyer et al., 2011). Here, we identified partially reprogrammed cells by cell-surface expression of TRA-1-60, a bona fide marker of fully reprogrammed cells (Chan et al., 2009). Twelve days after CD34$^+$ cells were transduced with Yamanaka factors, about 5% of total colonies expressed TRA1-60. These colonies represented fully reprogrammed cells (Lee et al., 2013). We also observed TRA1-60-negative colonies, with morphology similar to that of human ESCs (hESCs) but representing partially reprogrammed cells. We suggested that partially reprogrammed cells are "trapped" in an incompletely reprogrammed yet stable state not sufficient for full reprogramming (Chan et al., 2009; Lee et al., 2013).

We hypothesized that shifts in mitochondrial metabolic pathway checkpoints might be central to early stages of reprogramming prior to full pluripotency induction. Evidence for this exists (Folmes et al., 2011; Panopoulos et al., 2012; Xu et al., 2013), but detailed molecular mechanisms are lacking. MicroRNAs (miRNAs) regulate biological processes including embryonic development and somatic cell reprogramming (Anokye-Danso et al., 2011; Bang and Carpenter, 2008; Bartel, 2004). Among miRNAs

upregulated in fully reprogrammed iPSCs (Lee et al., 2013), we focused on miRNA 31 (miR-31), which is involved in cell proliferation (Slaby et al., 2007), migration (Valastyan et al., 2009), apoptosis (Bhatnagar et al., 2010), and differentiation (Deng et al., 2013). We postulated a role for miR-31 in metabolic transition to fully programmed iPSCs (fulliPSCs). Using bioinformatics, luciferase reporter assays, and overexpression experiments, a highly conserved binding site for miR-31 was predicted in the 3′ UTR of succinate dehydrogenase (succinate dehydrogenase complex subunit A; SDHA), which is part of the mitochondrial respiratory chain complex II and is encoded by nuclear DNA (Grimm, 2013), and participates in electron transfer in the respiratory chain and succinate catabolism in the Krebs cycle (Kim et al., 2012). Mutations in SDHA are rare but are linked to severe metabolic disorders resulting from decreased Krebs cycle activity, impaired oxidative phosphorylation, and bioenergetic deficiency. In contrast to other SDHs, inhibition of SDHA does not increase production of ROS under conditions of normal O_2 tension (normoxia), suggesting that reduction of SDHA activity might be an ideal way to reduce mitochondrial ETC activity, thus promoting fulliPSC induction while maintaining low ROS generation (Guzy et al., 2008). Evaluating metabolism of iPSCs without dissecting fully from partially reprogrammed iPSCs (pariPSCs), where the partially reprogrammed cells represent a majority of iPSCs, does not allow accurate evaluation of regulation of fulliPSC metabolism. We identified an miR-31/SDHA axis involvement in conversion of somatic cells to fulliPSCs, delineating a previously unrecognized role for miR-31 in regulating mitochondrial metabolism through suppressing SDHA during reprogramming. This may serve as a stratagem to more efficiently generate fulliPSCs for potential therapeutic use.

RESULTS

PariPSC Mitochondria Are Distinct from Those in FulliPSCs

PariPSCs are trapped in a stable intermediate reprogramming state (Chan et al., 2009; Mikkelsen et al., 2008). Although additional stem cell-related gene regulation is required to somehow overcome this barrier for transition to pluripotency (Mikkelsen et al., 2008), fulliPSCs and pariPSCs have not been well characterized for metabolic differences. We have now evaluated this for mitochondrial dynamics and respiration/oxygen consumption rates (OCR). Although there are no distinct differences in colony morphology between fully and partially reprogrammed cells (Figure 1A), all cells within fulliPSC colonies exhibited endogenous expression of OCT4, NANOG, SSEA4, and TRA-1-60 at levels similar to those of hESCs (Figure 1B, upper panel). Few cells within pariPSC colonies expressed these proteins (Figure 1B, lower panel).

We separately cultured and characterized pariPSCs and fulliPSCs using live TRA1-60 cell staining (Lee et al., 2013). pariPSCs ($GFP^-/TRA1\text{-}60^-$) had suppressed endogenous pluripotency gene expression as well as exogenous pluripotent gene expression (Figure S1A). Total and mitochondria-linked portions of total basal OCR, using a Seahorse Extracellular Flux analyzer, was greater in pariPSCs than in fulliPSCs, as was ATP-linked OCR, suggesting that pariPSCs are more dependent on mitochondrial respiration for their bioenergetic needs than fulliPSCs (Figure 1C). Treatment with the protonophore FCCP (carbonylcyanide p-trifluoromethoxyphenylhydrazone) had little effect on OCR in pariPSCs and fulliPSCs, consistent with ESCs having more "uncoupled" ETC than early differentiated ESCs, potentially due to increased uncoupling of protein-2 expression (Zhang et al., 2011); i.e., OXPHOS is more uncoupled from electron transport through the ETC and its subsequent translocation of protons and generation of proton motive force. Lower mitochondrial respiration in fulliPSCs could also be due to developmental immaturity of mitochondria. Structural/morphological changes in mitochondria, as well as function, are thought to be an absolute requirement for somatic cell reprogramming to iPSCs (Folmes et al., 2012; Xu et al., 2013). Using electron microscopy, the majority of mitochondria in fulliPSCs were rounded to oval, while those of pariPSCs were more elongated and enlarged with more defined cristae (Figure 1D), demonstrating that mitochondria in fulliPSCs are more immature in appearance than in pariPSCs. fulliPSCs had lower mitochondrial mass and decreased mitochondrial membrane potential compared with pariPSCs, and pariPSCs had elevated ROS levels (Figures 1E and 1F). This indicates preference for mitochondrial respiration in pariPSCs to support their bioenergetic needs.

PariPSCs and FulliPSCs Display Distinct Mitochondrial Gene and miRNA Profiles

FulliPSCs have a very different mitochondrial phenotype from pariPSCs, which could account for the higher mitochondrial respiration of pariPSCs. We examined mitochondrial gene-expression microarrays and found that a majority of genes coding for components of mitochondrial complex II and IV are more highly expressed in pariPSCs (Figure 2A and Table S1). SDHA was expressed at very low levels in human ESCs (hESC-H9), iPSCs (CB fulliPSC and fibro-fulliPSC), and embryonic carcinoma cells (ECCs; hECC-NT2), but was significantly increased in differentiated somatic cells (CB), pariPSCs (CB-partial cell and fibro-partial cell), and hESC-derived embryoid bodies (hESC-EB) especially when compared with the relative

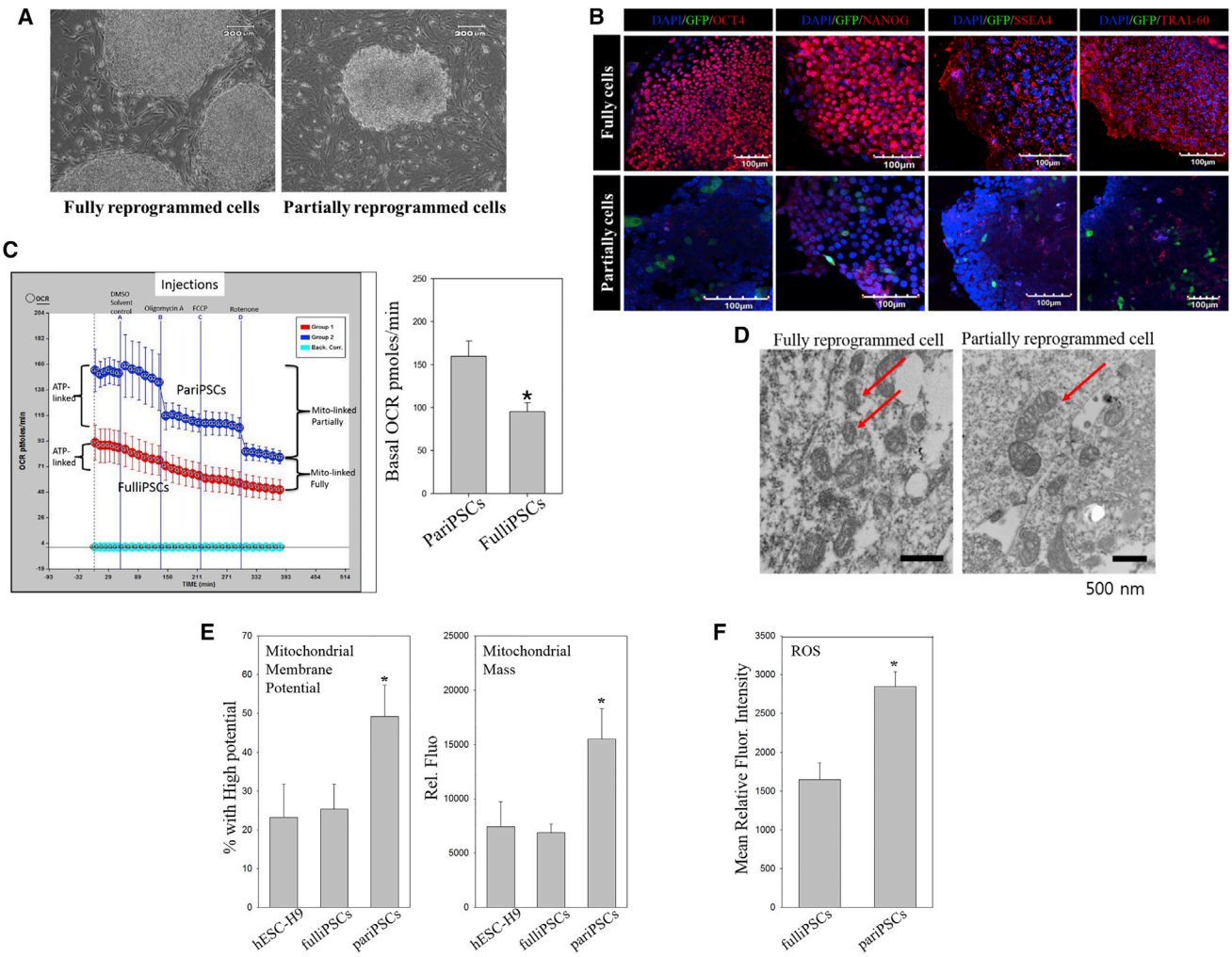

Figure 1. Differential Mitochondrial Characteristics in Partially Compared with Fully Reprogrammed iPSCs

(A) Microscope images of pariPSCs and fulliPSCs. Scale bars, 200 μm.

(B) Expression of exogenous GFP (green) and hESC-specific marker genes (red) OCT4, NANOG, SSEA4, and TRA1-60 in iPSCs by immunofluorescence analyses. Nuclei were counterstained with DAPI (blue). Scale bars, 100 μm.

(C) Average OCR measured before and after the indicated treatments. Mean basal OCR ± SD is the average of three independent experiments. Student's t test: *$p < 0.05$.

(D) Electron micrographs of mitochondria in pariPSCs and fulliPSCs. Arrows indicate mitochondria. Scale bars, 500 nm.

(E) Quantitative analysis comparing mitochondrial membrane potential by JC-1 and mitochondrial mass by Mitotracker Green FM staining in hESCs, and fulliPSCs and pariPSCs. The results represent the mean ± SD of four independent experiments performed in triplicate. Student's t test: *$p < 0.05$.

(F) Intracellular ROS quantitation in fulliPSCs and pariPSCs stained with Mitotracker Orange and assessed by flow cytometry. The results represent the mean ± SD of four independent experiments performed in triplicate. Student's t test: *$p < 0.05$.

expression abundance of the mitochondrial gene, COX-4, as well as with cytosolic β-actin (Figure 2B). We found that OCT4 and SDHA are mutually exclusive in pariPSCs and fulliPSCs.

This questions how mitochondrial gene changes occur during reprogramming. Understanding molecular mechanisms responsible for this blockage could aid in improving reprogramming efficiency. Metabolic remodeling occurs early in reprogramming (Figure 2) (Hansson et al., 2012; Varum et al., 2011); blocks to complete reprogramming in pariPSCs could involve further modification of mitochondrial characteristics needed for progression to full-iPSCs. We hypothesized that miRNAs play an important role in differential mitochondrial characteristics, and

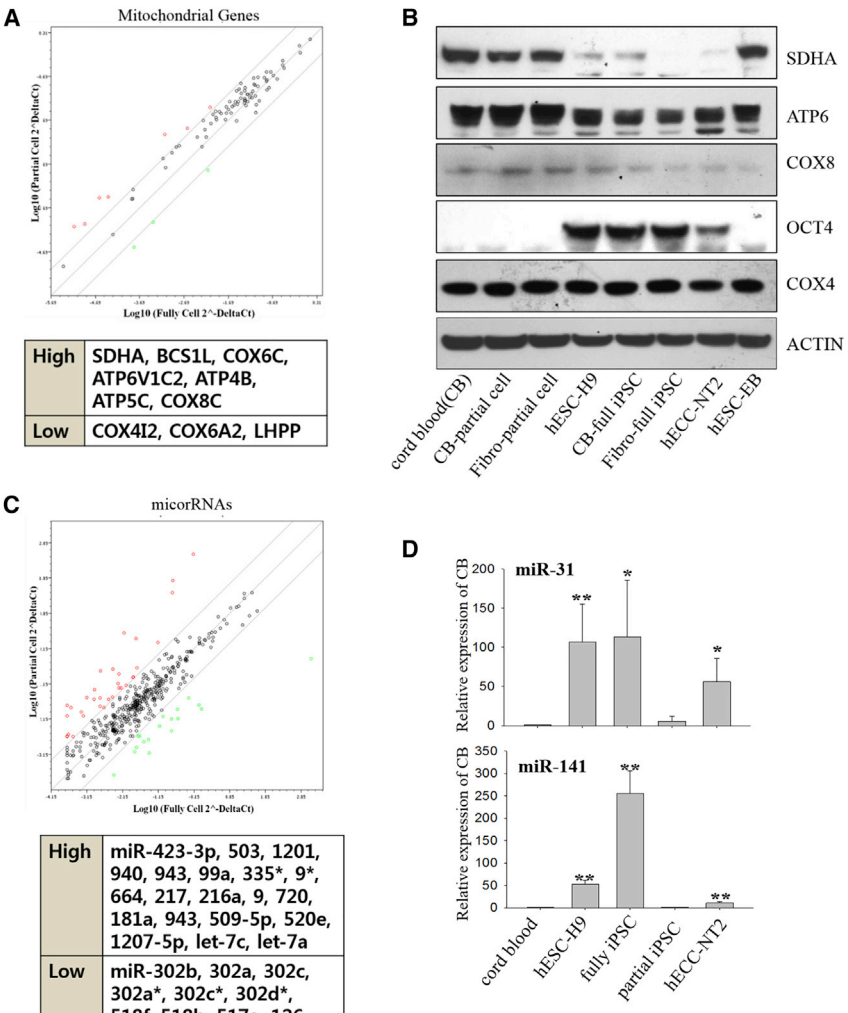

High	SDHA, BCS1L, COX6C, ATP6V1C2, ATP4B, ATP5C, COX8C
Low	COX4I2, COX6A2, LHPP

High	miR-423-3p, 503, 1201, 940, 943, 99a, 335*, 9*, 664, 217, 216a, 9, 720, 181a, 943, 509-5p, 520e, 1207-5p, let-7c, let-7a
Low	miR-302b, 302a, 302c, 302a*, 302c*, 302d*, 518f, 518b, 517a, 126, 205, 31, 200c, 141-3p,

Figure 2. Differential Mitochondrial Gene and miRNA Profiles

(A) Scatterplot compares normalized expression of mitochondria-related genes by plotting pariPSCs against fulliPSCs. The green dots indicate mitochondrial genes with ≥5-fold decrease in the relative expression in pariPSC compared with fulliPSC. The red dots indicate genes with ≥5-fold increase in the relative expression in pariPSC compared with fulliPSC. Lower panel shows list of genes whose expression changes >5-fold.

(B) Expression levels of proteins in CB cells, hESCs, fulliPSCs, pariPSCs, and hECCs assessed by western blotting.

(C) Scatterplot of miRNA PCR array. The green dots indicate miRNSs with ≥5-fold decrease in the relative expression in pariPSC compared with fulliPSC. The red dots indicate genes with ≥5-fold increase in the relative expression in pariPSC compared with fulliPSC. Lower panel shows list of miRNAs with high and low expression in pariPSCs.

(D) Individual PCR reactions normalized against U6 and plotted relative to expression level in CB cells. The results represent the mean ± SD of four independent experiments performed in triplicate. Student's t test: *$p < 0.05$ and **$p < 0.01$.

carried out miRNA PCR-array analysis (Lee et al., 2013). pariPSCs were markedly different from fulliPSCs in miRNA expression profiles (Figure 2C). To narrow the list of putative miRNAs that can regulate highly expressed genes in pariPSCs, we analyzed in silico algorithms using TargetScan (ver.5.1). We further restricted putative targets to those potentially associated with downregulated mitochondrial-specific genes in fulliPSCs. We focused on miR-31 and miR-141 from a list of low-expression miRNAs in pariPSCs that have the potential to bind SDHA, COX8, and ATP6V1C2, a vacuolar-type H^+-ATPase (V-ATPase) C2 subunit gene. fulliPSCs expressed much higher levels of miR-31 and miR-141 than pariPSCs (Figure 2D). We hypothesized that these candidate miRNAs might be involved in overcoming a conversion barrier from pariPSCs to fulliPSCs via regulation of mitochondrial metabolism by suppressing mitochondrial gene expression and activity.

SDHA, a Bona Fide Direct Target of miR-31

To identify bona fide miRNA targets among those predicted, we generated wild-type 3′ UTR (WT) and mutated 3′ UTR (Mut) Renilla luciferase reporter constructs (psi-check-2). SDHA containing Renilla luciferase activity was significantly downregulated compared with control (Figure 3A). In contrast, activities were not altered in the presence of COX8 and ATP6V1C-containing constructs, which were predicated as miR-141 putative targets. Together with bioinformatics predictions, downregulation of luciferase activity of SDHA by miR-31, and protein expression levels of SDHA (Figure 2B), this demonstrated that miR-31 represses gene expression by recognizing the predicted target sequence in the 3′ UTR of SDHA.

To determine whether downregulation of SDHA in pariPSCs could be due to miR-31, we overexpressed miR-31 in pariPSCs. We confirmed the expression level of miR-31

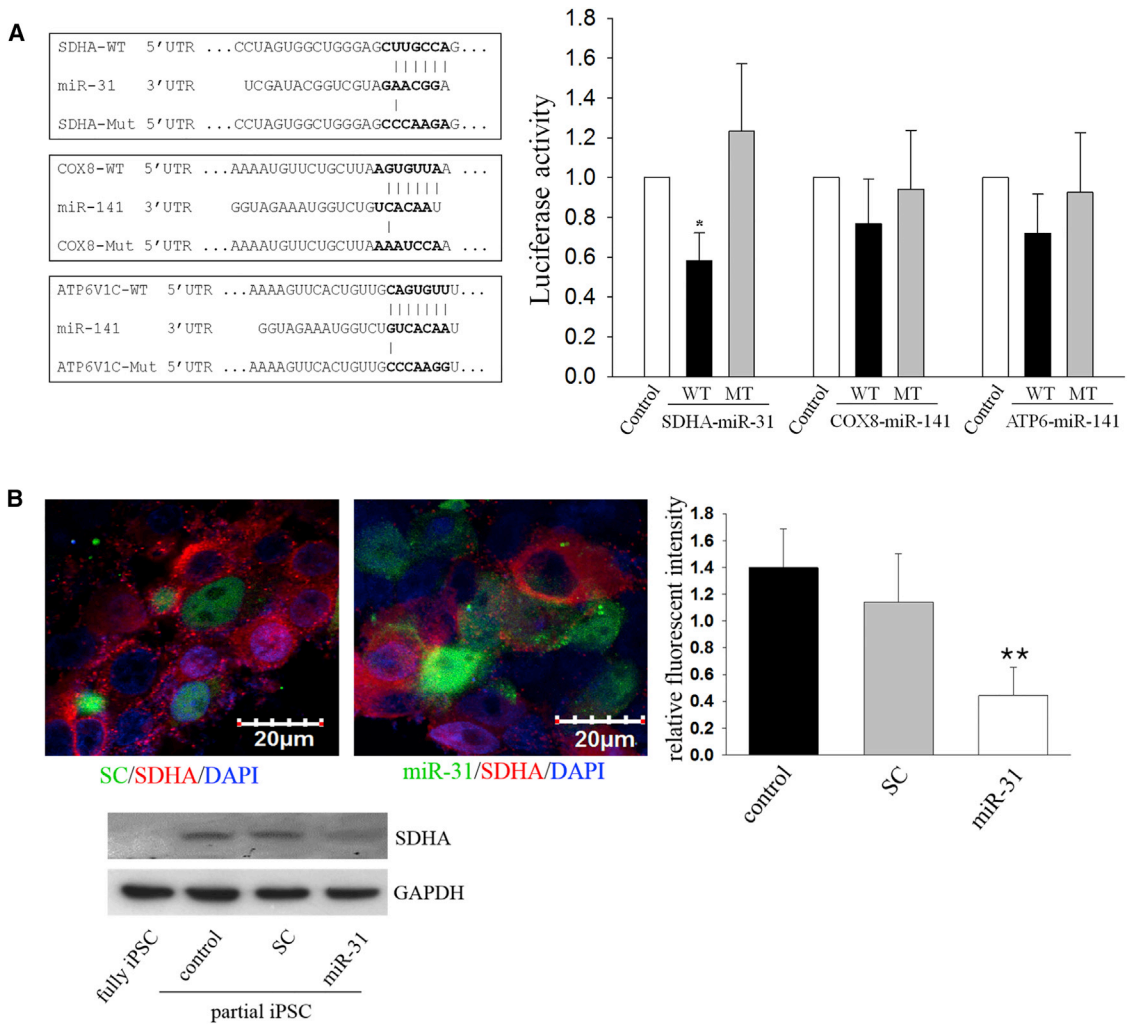

Figure 3. SDHA Is a Bona Fide Direct Target of miR-31

(A) Vector alone (control) or luciferase reporter constructs containing WT 3′ UTR of SDHA, ATPase6, or COX8 (WT) or mutant 3′ UTR (Mut) were co-transfected in the presence of miRNA oligomers to hECCs. Effects of miR-31 and miR-141 on relative luciferase activities are presented as histograms. The histogram represents the mean ± SD of three independent experiments performed in triplicate. Student's t test: *$p < 0.05$.

(B) Expression of SDHA with miR-31 is shown in upper panels (immunostaining) and western blotting in the lower panel. The bar chart presents relative fluorescence intensity of SDHA and represents the mean ± SD of three independent experiments. Student's t test: **$p < 0.01$.

in pariPSC transduced with lentiviral construct with miR-31 gene by qPCR (Figure S1B). Using confocal microscopy, pariPSCs transduced with a scramble control construct showed widespread punctate expression of SDHA, whereas miR-31-overexpressing cells had reduced SDHA expression (Figure 3B). pariPSCs transduced with miR-31 had significantly decreased SDHA protein expression by western blot (Figure 3B, bottom panel). This level in miR-31-overexpressing cells was similar to that in fulliPSCs. Thus, down-regulated miR-31 expression results in increased SDHA expression in pariPSCs.

MiR-31 Overexpression Modulates Metabolic Functions by Suppressing SDHA Activity

To ensure a functional connection with miR-31 and SDHA complex II enzyme activity, we transduced miR-31 or short hairpin RNA (shRNA)-SDHA into human CB-CD34$^+$ cells and measured in vitro enzyme activity of ETC complex II SDHA in pariPSCs overexpressing miR-31 (Figures 4A, S2A, and S2B). Complex II activity in pariPSCs overexpressing miR-31 was reduced 45.3% compared with fulliPSCs. Inhibition of SDHA by shRNA also decreased complex II activity by greater than 56.1% (Figure 4A). Thus, miR-31

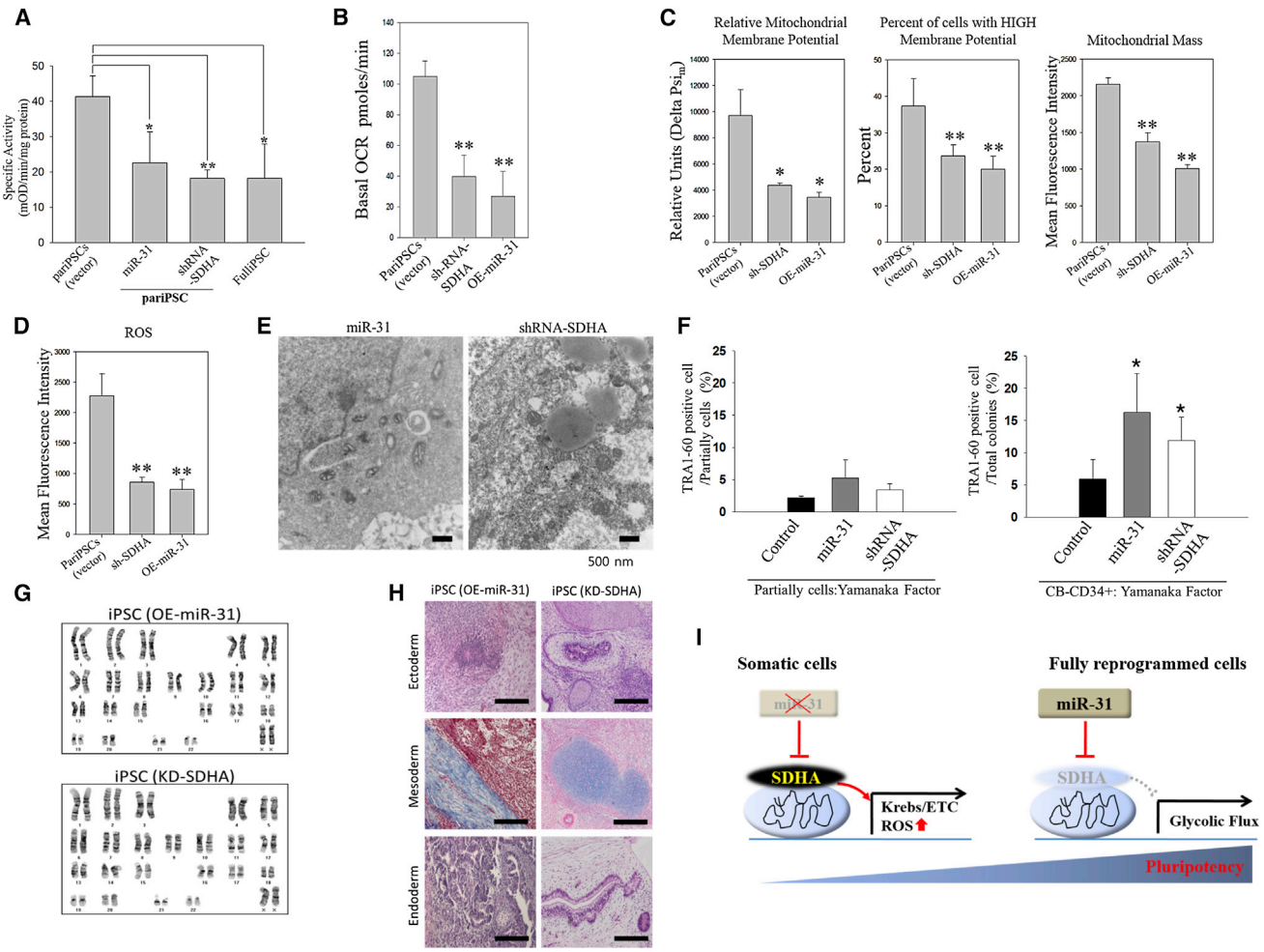

Figure 4. MiR-31 and shRNA-SDHA Increase Complete Reprogramming

(A) ETC complex II activity assays showing miR-31 and shRNA-SDHA represses complex II activity by approximately 50%. y Axis represents rate, which is the difference in the absorbance divided by time and normalized to total protein. The results represent the mean ± SD of three independent experiments performed in triplicate. Student's t test: *$p < 0.05$ and **$p < 0.01$.

(B) Basal OCR measured by respirometry. The results represent the mean ± SD of three independent experiments performed in triplicate. Student's t test: **$p < 0.01$.

(C) Relative mitochondrial membrane potential and percentage of cells with high membrane potential, and mitochondrial mass. The results represent the mean ± SD of three independent experiments performed in triplicate. Student's t test: *$p < 0.05$ and **$p < 0.01$.

(D) Relative mitochondrial ROS levels. The results represent the mean ± SD of three independent experiments performed in triplicate. Student's t test: **$p < 0.01$.

(E) Electron microscopy of mitochondria in miR-31 and shRNA-SDHA pariPSCs. Scale bars, 500 nm.

(F) miR-31 and shRNA-SDHA pariPSCs (left panel) or CB-CD34$^+$ cells with Yamanaka factors (right panel) analyzed by fluorescence-activated cell sorting for expression of TRA-1-60. The results represent the mean ± SD of three independent experiments for each miR-31 and shRNA transduction performed in triplicate. Student's t test: *$p < 0.05$.

(G) Karyotyping analysis in fully reprogrammed iPSCs generated by co-infection OE-miR-31 and KD-SDHA with Yamanaka factor in CB-CD34$^+$ cells revealed normal chromosomal stability.

(H) Teratomas derived from immunodeficient mice injected with fully reprogrammed iPSCs generated by co-infection OE-miR-31 and KD-SDHA with Yamanaka factor in CB-CD34$^+$ cells miR-302-iPS cells show tissues representing all three embryonic germ layers, including respiratory tract (endoderm), cartilage (mesoderm), and secretory epithelium or neural rosette (ectoderm). Scale bars, 50 μm.

(I) Proposed mechanism showing that miR-31/SDHA axis acts as a master switch for pluripotent metabolic reprogramming.

suppresses mitochondrial complex II activity via suppression of SDHA transcription.

We measured mitochondrial respiration in lentiviral miR-31 overexpression or shRNA-SDHA-treated pariPSCs to explore a link between miR-31 and activity of the SDHA complex II enzyme in regulating metabolism. Both shRNA-SDHA and lentiviral miR-31 led to a reduction of basal OCR of 62% and 72%, respectively, similar to levels in fulliPSCs (Figure 4B). ShRNA-SHDA and overexpressed miR-31 reduced mitochondrial membrane potential, mitochondrial mass, and ROS levels (Figures 4C and 4D). Mitochondrial membrane potential and ROS production, assayed by JC-9 and DCF-DA, respectively, displayed similar patterns (Figure S3A). To further define pariPSCs we assessed the levels of succinate and fumarate, mitochondrial substrates produced by Krebs cycle reaction (Figure S3B). Partially reprogrammed cells significantly accumulated levels of succinate similar to those from fully reprogrammed cells. Overexpression of miR-31 or shRNA-SDHA into pariPSC increased succinate levels almost to levels of fulliPSCs, indicating that miR31 promotes reprogramming by attenuating mitochondrial complex II function. Reduced ROS generation is consistent with diminished mitochondrial ETC activity and is a critical factor in maintaining pluripotency (Han et al., 2008). Compared with mitochondrial morphology of pariPSCs, the morphology of lentiviral miR-31 or shRNA-SDHA-treated pariPSCs was a more immature round shape, consistent with mitochondria found in PSCs and non-transduced fulliPSCs (Figure 4E). This indicates that the miR-31-SDHA axis might also be correlated with mitochondrial biogenesis/dynamics as well as the reprogramming process.

Early Overexpression of MiR-31 or shRNA-SDHA Is Required for Full Reprogramming

We investigated when transduction of miR-31 and shRNA-SDHA was required for maximal Tra1-60 induction. We transduced miR-31 or shRNA-SDHA into $CD34^+$ starting cells and into pariPSCs and compared expression levels of TRA1-60, a marker for fulliPSC (Figure 4F). CB-$CD34^+$ cells transduced with lentiviral miR-31 induced TRA1-60 by 2.7-fold compared with control cells (Figure 4F, right panel), while transduced, pariPSCs did not show increased expression of TRA1-60 (Figure 4F, left panel). Effects of transduced shRNA-SDHA on TRA1-60 induction was observed only in $CD34^+$ cells but not in pariPSCs after reprogramming culture, indicating that miR-31 or shRNA-SDHA exerted maximal effects only when introduced to the cells at an early stage of reprogramming. Reprogramming proceeds through a series of stages, but the majority of cells are trapped by transition barriers, generating intermediate cells as a transition state during reprogramming. Downmodulation of SDHA may be necessary to lower the threshold of such barriers to improve reprogramming efficiency before cells undertake remodeling of epigenetic marks, such as DNA methylation, for transition to a fulliPSC stage.

Karyotype assay indicated no sign of chromosomal abnormality in iPSCs derived from cells transduced with miR-31 or shRNA-SDHA (Figure 4G). TRA1-60^+ cells derived from CB-$CD34^+$ cells overexpressing miR-31 or shRNA-SDHA developed teratomas containing three germ-cell layers, a trait of iPSCs and PSCs (Figure 4H). Thus, upregulation of miR-31 improves reprogramming efficiency without altering prototype iPSC characteristics.

We have demonstrated that miR-31 may play an important role in improving reprogramming efficiency by lowering thresholds of transition stages, likely by remodeling mitochondria through SHDA, a critical enzyme for mitochondrial functions, acting at early stages of the reprogramming process.

DISCUSSION

Yamanaka factors induce somatic cell reprogramming to iPSCs by promoting spatiotemporal expression of PSC-specific and metabolic genes. However, only a small fraction of these cells complete full reprogramming, leaving most cells at an intermediate stage (Chan et al., 2009; Lee et al., 2013; Mikkelsen et al., 2008), suggesting that cells remaining at an intermediate stage may be restricted by a "reprogramming checkpoint." Mitochondrial reprogramming may be coupled with cell-fate conversion (Buganim et al., 2013; Hansson et al., 2012). We termed these intermediate cells collectively as pariPSCs, with distinguishing characteristics. (1) Unlike somatic cells, pariPSCs formed colonies similar to those of fully reprogrammed cells (Figures 1A and 1B). (2) However, pariPSCs differed from fulliPSCs in mitochondrial functions. (3) pariPSCs did not express pluripotent-specific genes such as TRA1-60, or endogenous OCT4 and SOX2, which are abundantly expressed in fulliPSCs (Figure 1B). (4) pariPSCs resembled fulliPSCs with regard to self-renewal potential, as they multiplied up to at least 20 passages without losing their phenotypes. (5) However, pariPSCs were not simply transformed cells sporadically generated during reprogramming, as manifested by their inability to form teratomas in vivo when implanted into mice (Lee et al., 2013). (6) Unlike somatic cells, pariPSCs studied here possessed the same feature as fulliPSCs in the ability to silence exogenously transduced genes. Taking all of these unique characteristics of these cells into consideration, we referred to TRA1-60^- and GFP^- cells as pariPSCs.

Molecular mechanisms involved in reprogramming somatic cells to fulliPSC by Yamanaka factors remain largely enigmatic, particularly with respect to the mitochondrial

metabolic shift from respiration-dependent bioenergetic to more glycolytic pathways. PariPSCs and fulliPSCs were quite different in expression levels of miR-31 and SDHA, a flavoprotein subunit of mitochondria complex II and vital for the Krebs cycle. MiR-31 was expressed in pariPSCs and somatic cells at minimal levels, but was expressed abundantly in fulliPSCs and PSCs. Opposite to miR-31, SDHA was found in pariPSCs and somatic cells at high levels, but at low levels in fulliPSCs and ESCs. Reciprocal expression between miR-31 and SDHA in pariPSCs and fulliPSCs led us to speculate that SDHA might be a regulatory target for miR-31. MiR-31 transduction greatly suppressed SDHA expression (Figure 3), and miR-31 and shRNA-SDHA had similar roles in reducing mitochondrial activities. Importantly, miR-31 or shRNA-SDHA markedly increased cell populations expressing TRA1-60, a marker for ESCs and fully reprogrammed cells, when transduced into CB-CD34$^+$ cells (Figure 4F). Transduction of miR-31 or shRNA-SDHA in pariPSCs was not as apparent for inducing TRA1-60 expression as seen in CB-CD34$^+$ cells (Figure 4F). This suggests that miR-31 should reside in cells at early stages of reprogramming to efficiently improve reprogramming. Early appearance of miR-31 (in this case CB-CD34$^+$ cells) may equip cells in a more favorable intracellular environment to downmodulate mitochondrial ETC activity and alter mitochondrial features such as ROS generation, membrane potential, and mass.

It is unclear whether altered function of mitochondrial metabolites actually mediates the effects of miR-31 and shRNA-SDHA on increasing reprogramming efficiency. We carried out experiments to trace glucose metabolites after transduction with miR-31 or shRNA-SDHA by using ^{13}C-labeled glucose. Unfortunately, ^{13}C radioactivity of mitochondrial metabolites was too low to detect due to the high content of glucose existing in reprogramming culture medium. We evaluated whether changes in mitochondrial levels of succinate and fumarate, respective substrates and products of SDHA, affected reprogramming efficiency. While overexpression of miR-31 or shRNA-SDHA in partially reprogrammed cells significantly increased succinate levels, almost to that of fully reprogrammed iPSCs (data not shown), this did not significantly change reprogramming efficiency (data not shown). We tried to knock down SDHB using shRNA to reveal the reprogramming effects of other subunits of the succinate dehydrogenase complex. Because SDHA and SDHB compose hydrophilic subunits of respiratory complex II in the inner mitochondrial membrane, we expected that SDHB might have the potential to regulate reprogramming. However, we did not see any effects of SDHB-shRNA. We suspect that SDHB protein might have a slower turnover of translation or that shRNA might not work strongly on the exact target sequence of SDHB. Regardless, since transduction of shRNA-SDHA resulted in attenuation of mitochondrial functions, this most likely facilitates an environment favorable for reprogramming.

Theoretically, enhanced induction of TRA1-60, a specific marker for reprogrammed iPSCs by miR-31 and shRNA-SDHA, can be achieved in two ways: improved reprogramming efficiency or inhibiting pariPSCs from differentiating back into somatic cells. We strongly favor the view that enhanced induction of TRA1-60 by miR-31 and shRNA-SDHA resulted from improved reprogramming efficiency. Thus far, we have no evidence that pariPSCs differentiate back into the original CD34$^+$ cells they were derived from, or any other type of somatic cells, in the presence of Yamanaka factors.

Control of mitochondrial SDHA expression through miR-31 may be a way to increase reprogramming efficiency at early reprogramming stages. This underlies the importance of SDHA and miR-31 for establishing a better understanding of miRNA mitochondria-related molecular mechanisms for reprogramming.

EXPERIMENTAL PROCEDURES

All human studies were performed with the approval of an Institutional Review Board from the Indiana University School of Medicine (IUSM) (IRB No. 1011002987) and Konkuk University Hospital (IRB No. KUH 1280081). All animal experiments were performed in compliance with the Institutional Animal Care and Use Committee of the IUSM (IACUC No. 10985 MD/R/E/AR) and Konkuk University (IACUC No. KU15151-1) and the Guidelines for the Care and Use of Laboratory Animals of the National Research Council.

Complex II Activity

Complex II activity was assessed following manufacturer's instructions (Abcam) (Grosso et al., 2013).

Respirometry

Respirometry analysis was performed with a Seahorse XF96 extracellular flux analyzer as reported by Grosso et al. (2013).

Procedures for maintenance of hESC and hiPS, qRT-PCR for miRNA, immunocytochemistry, western blotting, 3′ UTR luciferase reporter assays, teratoma assay, and flow cytometry analysis have been reported by us previously (Lee et al., 2013). Full details are provided in Supplemental Experimental Procedures.

Statistical Analysis

All experiments were performed three times in triplicate, and data are represented as mean ± SD for statistical comparison. Significance of differences was assessed by an unpaired t test at $p < 0.05$.

SUPPLEMENTAL INFORMATION

Supplemental Information includes Supplemental Experimental Procedures, three figures, and one table and can be found

with this article online at http://dx.doi.org/10.1016/j.stemcr.2016.05.012.

AUTHOR CONTRIBUTIONS

M.R.L. and C.M.: conception and design, collection and/or assembly of data, data analysis and interpretation, and manuscript writing; S.A.L. and S.H.M.: collection and assembly of data; H.E.B.: conception and design, financial support, manuscript writing, and final approval of manuscript.

ACKNOWLEDGMENTS

These studies were supported by Public Health Service grants RO1 HL056416, RO1 HL67384, RO1 HL112669, and PO1 DK090948/U54 DK106846 from the NIH to H.E.B., the Korea Health Technology R&D Project (KHIDI) funded by the Ministry of Health & Welfare, Republic of Korea (HI14C2755020014), and the Basic Science Research Program through the National Research Foundation of Korea (NRF) funded by the Ministry of Education (2015R1A6A1A03032522).

Received: October 28, 2015
Revised: May 27, 2016
Accepted: May 31, 2016
Published: June 23, 2016

REFERENCES

Anokye-Danso, F., Trivedi, C.M., Juhr, D., Gupta, M., Cui, Z., Tian, Y., Zhang, Y., Yang, W., Gruber, P.J., Epstein, J.A., et al. (2011). Highly efficient miRNA-mediated reprogramming of mouse and human somatic cells to pluripotency. Cell Stem Cell *8*, 376–388.

Bang, A.G., and Carpenter, M.K. (2008). Development. Deconstructing pluripotency. Science *320*, 58–59.

Bartel, D.P. (2004). MicroRNAs: genomics, biogenesis, mechanism, and function. Cell *116*, 281–297.

Bhatnagar, N., Li, X., Padi, S.K.R., Zhang, Q., Tang, M.S., and Guo, B. (2010). Downregulation of miR-205 and miR-31 confers resistance to chemotherapy-induced apoptosis in prostate cancer cells. Cell Death Dis. *1*, e105.

Broxmeyer, H.E., Lee, M.R., Hangoc, G., Cooper, S., Prasain, N., Kim, Y.J., Mallett, C., Ye, Z., Witting, S., Cornetta, K., et al. (2011). Hematopoietic stem/progenitor cells, generation of induced pluripotent stem cells, and isolation of endothelial progenitors from 21- to 23.5-year cryopreserved cord blood. Blood *117*, 4773–4777.

Buganim, Y., Faddah, D.A., and Jaenisch, R. (2013). Mechanisms and models of somatic cell reprogramming. Nat. Rev. Genet. *14*, 427–439.

Chan, E.M., Ratanasirintrawoot, S., Park, I.-H., Manos, P.D., Loh, Y.-H., Huo, H., Miller, J.D., Hartung, O., Rho, J., Ince, T.A., et al. (2009). Live cell imaging distinguishes bona fide human iPS cells from partially reprogrammed cells. Nat. Biotechnol. *27*, 1033–1037.

Deng, Y., Wu, S., Zhou, H., Bi, X., Wang, Y., Hu, Y., Gu, P., and Fan, X. (2013). Effects of a miR-31, Runx2, and Satb2 regulatory loop on the osteogenic differentiation of bone mesenchymal stem cells. Stem Cell Dev. *22*, 2278–2286.

Folmes, C.D., Nelson, T.J., Martinez-Fernandez, A., Arrell, D.K., Lindor, J.Z., Dzeja, P.P., Ikeda, Y., Perez-Terzic, C., and Terzic, A. (2011). Somatic oxidative bioenergetics transitions into pluripotency-dependent glycolysis to facilitate nuclear reprogramming. Cell Metab. *14*, 264–271.

Folmes, C.D., Dzeja, P.P., Nelson, T.J., and Terzic, A. (2012). Metabolic plasticity in stem cell homeostasis and differentiation. Cell Stem Cell *11*, 596–606.

Grimm, S. (2013). Respiratory chain complex II as general sensor for apoptosis. Biochim. Biophys. Acta *1827*, 565–572.

Grosso, S., Doyen, J., Parks, S.K., Bertero, T., Paye, A., Cardinaud, B., Gounon, P., Lacas-Gervais, S., Noel, A., Pouyssegur, J., et al. (2013). MiR-210 promotes a hypoxic phenotype and increases radioresistance in human lung cancer cell lines. Cell Death Dis. *4*, e544.

Guzy, R.D., Sharma, B., Bell, E., Chandel, N.S., and Schumacker, P.T. (2008). Loss of the SdhB, but Not the SdhA, subunit of complex II triggers reactive oxygen species- dependent hypoxia-inducible factor activation and tumorigenesis. Mol. Cell Biol. *28*, 718–731.

Han, M.-K., Song, E.-K., Guo, Y., Ou, X., Mantel, C., and Broxmeyer, H.E. (2008). SIRT1 regulates apoptosis and Nanog expression in mouse embryonic stem cells by controlling p53 subcellular localization. Cell Stem Cell *2*, 241–251.

Hansson, J., Rafiee, M.R., Reiland, S., Polo, J.M., Gehring, J., Okawa, S., Huber, W., Hochedlinger, K., and Krijgsveld, J. (2012). Highly coordinated proteome dynamics during reprogramming of somatic cells to pluripotency. Cell Rep. *2*, 1579–1592.

Kim, H.J., Khalimonchuk, O., Smith, P.M., and Winge, D.R. (2012). Structure, function, and assembly of heme centers in mitochondrial respiratory complexes. Biochim. Biophys. Acta *1823*, 1604–1616.

Lee, M.R., Prasain, N., Chae, H.D., Kim, Y.J., Mantel, C., Yoder, M.C., and Broxmeyer, H.E. (2013). Epigenetic regulation of NANOG by miR-302 cluster-MBD2 completes induced pluripotent stem cell reprogramming. Stem Cells *31*, 666–681.

Liu, W., Long, Q., Chen, K., Li, S., Xiang, G., Chen, S., Liu, X., Li, Y., Yang, L., Dong, D., et al. (2013). Mitochondrial metabolism transition cooperates with nuclear reprogramming during induced pluripotent stem cell generation. Biochem. Biophys. Res. Commun. *431*, 767–771.

Mikkelsen, T.S., Hanna, J., Zhang, X., Ku, M., Wernig, M., Schorderet, P., Bernstein, B.E., Jaenisch, R., Lander, E.S., and Meissner, A. (2008). Dissecting direct reprogramming through integrative genomic analysis. Nature *454*, 49–55.

Panopoulos, A.D., Yanes, O., Ruiz, S., Kida, Y.S., Diep, D., Tautenhahn, R., Herrerias, A., Batchelder, E.M., Plongthongkum, N., Lutz, M., et al. (2012). The metabolome of induced pluripotent stem cells reveals metabolic changes occurring in somatic cell reprogramming. Cell Res. *22*, 168–177.

Slaby, O., Svoboda, M., Fabian, P., Smerdova, T., Knoflickova, D., Bednarikova, M., Nenutil, R., and Vyzula, R. (2007). Altered

expression of miR-21, miR-31, miR-143 and miR-145 is related to clinicopathologic features of colorectal cancer. Oncology *72*, 397–402.

Valastyan, S., Reinhardt, F., Benaich, N., Calogrias, D., Szasz, A.M., Wang, Z.C., Brock, J.E., Richardson, A.L., and Weinberg, R.A. (2009). A pleiotropically acting microRNA, miR-31, inhibits breast cancer metastasis. Cell *137*, 1032–1046.

Varum, S., Rodrigues, A.S., Moura, M.B., Momcilovic, O., Easley, C.A.t., Ramalho- Santos, J., Van Houten, B., and Schatten, G. (2011). Energy metabolism in human pluripotent stem cells and their differentiated counterparts. PLoS One *6*, e20914.

Xu, X., Duan, S., Yi, F., Ocampo, A., Liu, G.H., and Izpisua Belmonte, J.C. (2013). Mitochondrial regulation in pluripotent stem cells. Cell Metab. *18*, 325–332.

Zhang, J., Khvorostov, I., Hong, J.S., Oktay, Y., Vergnes, L., Nuebel, E., Wahjudi, P.N., Setoguchi, K., Wang, G., Do, A., et al. (2011). UCP2 regulates energy metabolism and differentiation potential of human pluripotent stem cells. EMBO J. *30*, 4860–4873.

Zhang, J., Nuebel, E., Daley, G.Q., Koehler, C.M., and Teitell, M.A. (2012). Metabolic regulation in pluripotent stem cells during reprogramming and self-renewal. Cell Stem Cell *11*, 589–595.